EXPERIMENTAL STUDY OF A LARGE TEMPERATURE DIFFERENCE THERMAL ENERGY STORAGE TANK FOR CENTRALIZED HEATING SYSTEMS

by

Jian SUN [a*], ***Jing HUA*** [b], ***Lin FU*** [b], ***and Shigang ZHANG*** [b]

[a] School of Energy, Power, and Mechanical Engineering, North China Electric Power University, Beijing, China
[b] Department of Building Science, Tsinghua University, Beijing, China

Original scientific paper
https://doi.org/10.2298/TSCI160720173S

Decreasing the backwater temperature of the primary pipe in a centralized heating system is one successful way to increase the heating capacity and recover different kinds of industrial low-grade heat from the system. A new system combining an energy storage tank and a heat pump is introduced in this study as the key device in this system, so the temperature difference of this thermal storage tank could be over 25 °C. To improve the thermal energy storage tank design, a mathematical model considering disturbance factor is given, an experimental system is built, and good agreement is found when the experimental results are compared with simulation results.

Key words: *thermal energy storage, turbulence factor, thermocline*

Introduction

Energy and the environment have become two significant research areas in recent decades, and the use of different kinds of low-grade industrial heat is playing an increasingly more important role in recent studies [1].

Centralized heating systems also play a more important role in heating areas in that they are systems that allow for higher energy efficiency and lower air pollution than interurban heating [2].

An efficient and available way to increase energy efficiency and heating capacity of current heating pipes is the decreasing the temperature of primary pipe back water.

However, the backwater temperature of primary pipes could not be lower than that of the secondary pipe due to the necessary temperature difference. Meanwhile, absorption heat pumps are used at the thermal substation, which could make the working case temperature in the ranges of 120-30 °C for the primary pipe and 45-60 °C for the secondary pipe [3]. However, the backwater temperature of the primary pipe could only be decreased to a limited level by adopting an absorption heat pump. A heating network with a direct connection is quite difficult to operate and is not suitable for the large heating area. Furthermore, it is quite difficult to build new heating systems for a built city when considering required space for heating sources, required space and high cost for heating pipes, environmental protection and so on.

* Corresponding author, e-mail: s@ncepu.edu.cn

In this paper, due to its high performance, a compression heat pump is selected to significantly decrease the backwater temperature of the primary pipe, which is aimed to directly recover different kinds of industrial waste heat. However, the electrical consumption of this heat pump is large and it is expensive to operate. Meanwhile, electricity prices vary in most Chinese cities, and the price during the day may be more than three times greater than that at night in some cities. Therefore, a thermal storage tank is adopted in this system to reduce the electricity consumption of the compression heat pump.

Many efforts have been made for the installation of thermal energy storage (TES) tanks for district heating. The intermittent heat production characteristic from industrial excess heat, solar energy, and heat pumps justifies the implementation of TES in district heating systems. The TES can be divided into the two types: diurnal heat storage and seasonal storage [4].

The TES systems and combined heating and power (CHP) plants can balance energy demands and stabilize the electricity grid [5]. Expanded TES systems at a CHP plant allow for the highly flexible generation of electricity for increasing revenues and reducing the fuel consumption of peak load boilers [6]. The CHP with short-term sensible storage tanks in Sweden and Denmark enable plants to be designed smaller and to run at full capacity [7]. A comparison of a solar collector plant equipped with TES is discussed and is proved to be feasible, but considerable improvements need to be completed with respect to insulation [8].

A thermal substation system, as shown in fig. 1. This system significantly decreases the back water temperature of the primary pipe, increases the heating capacity of current heating pipe and decreases the heating cost by recovering different kinds of low-grade industrial waste heat.

To reduce the electrical consumption of this system, a thermal energy storage tank is employed, as shown in fig. 1. The electrical heat pump is powered on at night and hot water is cooled by the AHP, which is then cooled again with hot water storage in TES by the EHP. Meanwhile, the cooled water is divided into the two parts: one part is stored in the TES from the bottom and the other part enters into the primary pipe. The EHP is powered off during the day, and cold-water storage in the TES enters into the primary pipe, which maintains the low of backwater temperature of the primary pipe. Meanwhile, the TES is filled with the hot water from the AHP. Therefore, the TES could reduce the electrical consumption of this system by the price difference advantage of electricity during the day *vs*. at night, and the low return water temperature of the primary pipe could be continually maintained.

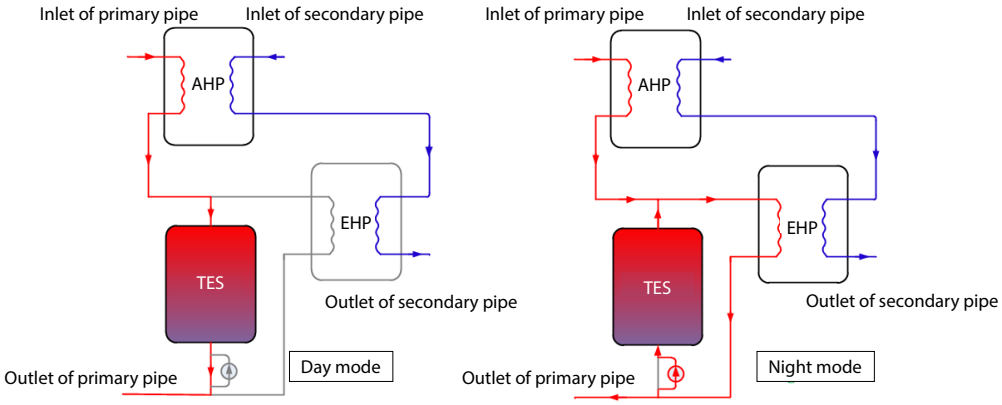

Figure 1. Combined thermal substation process

This research is focused on this TES, whose temperature difference is typically greater than 25 °C. However, TES is often adopted for chilled water and solar energy storage. The most effective technology for chilled water storage, both economically and thermodynamically, is a naturally stratified tank. Stratified tanks are always specified in virtually new installations [9].

To sufficiently store and use high-quality heat energy, thermal stratification is gradually applied in many kinds of energy storage fields such as solar thermal utilization systems [10].

Experimental system of the TES tank

The temperature difference of TES is often less than 10 °C when adopted for chilled water storage [10]. To investigate the heat transfer characteristic of TES with a large temperature difference, an experimental system with a TES tank is built and tested, as shown in fig. 2. The ratio of height to diameter could affect the temperature profile of the TES tank directly, and the ratio of the thickness of mixing layer in the overall height is reduced with a thin long tank. However, the pressure in the bottom of the tank is increased, which requires a thick tank wall for high bearing pressure. A TES tank 4 m in diameter and 7 m high is used considering the space of thermal substation.

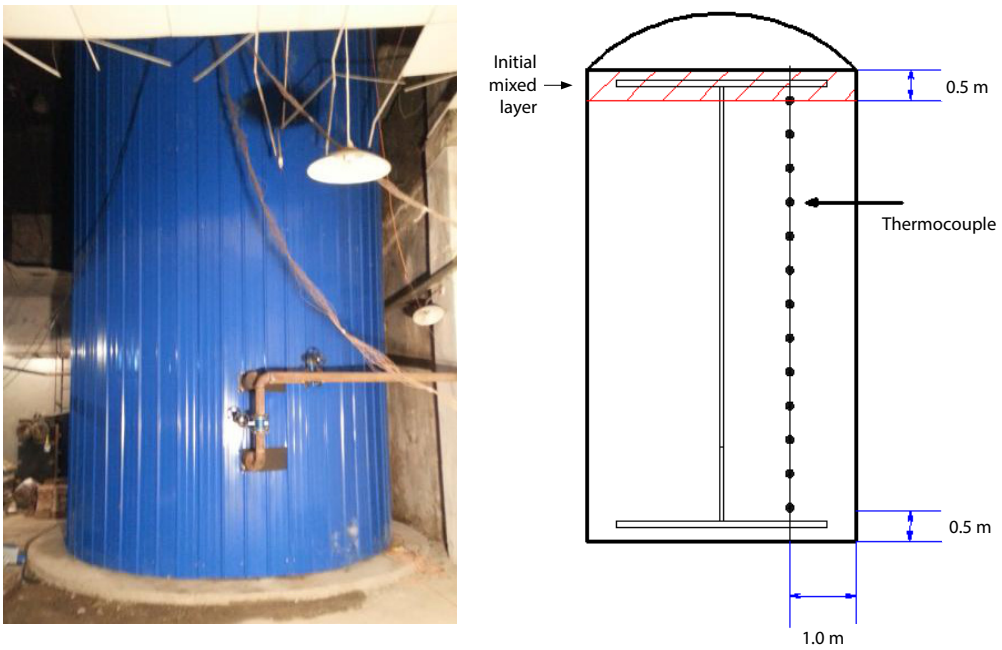

Figure 2. Initial mixed layer of the TES tank

Flow rates of the TES tank are automatically recorded by a magnetic-flow meter, which has an accuracy of 0.5%. Temperature sensors are installed at the inlets and outlet of the different units. All thermocouples (type T) are calibrated by the constant temperature oil bath with an accuracy of 0.1 °C. An Agilent data acquisition instrument (34970A) automatically records the data of all installed sensors. To measure the temperature at different heights inside the TES tank, 13 thermocouples are installed inside the tank with a vertical distance of 0.5 m. The first thermocouple is 0.5 m from the bottom of the tank, and the last thermocouple is 0.5 m from the top.

Mathematical models for TES tanks

There are some presented mathematical models for TES tanks. A review of the thermal stratification within the water tank is given. The relevant research methods are listed, and some stratification tank experiments are also compared [10]. A CFD method is adopted to determine the thermal stratification mechanism of the storage tank. The results show that the ideal type-plug flow model could be used as a possible tool for simulation with good stratification [11]. The influence of the inlet mass-flow rate on the degree of thermal stratification is analysed by CFD simulation, and the verification of solutions and post-processing tasks are calculated in order to quantify the level of thermal stratification [12]. A simple finite difference computer code is given with the flow governing conservation equations, and the results show that the effect of inlet geometry is weak for Richardson numbers above 10 [13]. A 2-D model is simplified for the pure conduction case, which emphasizes the key role of temperature profile conduction [14].

An experimental investigation is given for the chilled water storage system. The height and diameter of the tank are 1850 mm and 850 mm, respectively. Temperatures of hot water and chilled water are 17 °C and 4 °C, respectively. Thermal efficiency up to 90% could be achieved [15]. Several models are compared considering internal natural and mixed convection [16].

A 1-D model is used in TRNSYS to predict the temperature profile inside a stratified tank with multiple heat exchangers and compared the model with experimental results. The 1-D model includes the effects of mass transfer within the tank as well as mass-flow into and out of the tank, thermal de-stratification and heat loss to the ambient [17]. The model was used to validate the simplified model, who found that using 10 nodes is adequate to accurately predict transient energy storage capacity (with less than 2% error) [18].

The 1-D model does not capture the radial temperature gradient. However, experimental results from another study that considered a stratified tank with stored water-flow into and out of tank showed relatively negligible temperature variation in the radial direction [19].

This study is aimed at improving the 1-D model of a TES tank to analyse the turbulence effect on the temperature profile with a water distributor and a 1-D model with disturbance factor is presented. The hydrodynamic effect at the TES tank inlet is considered as exponential decay with time.

Based on the conduction equation, the heat storage process could be described:

$$\frac{\mathrm{d}T}{\mathrm{d}t}=\frac{\lambda}{\rho c_p}\frac{\partial^2 T}{\partial x^2}-v\frac{\partial T}{\partial x}+\frac{4K}{\rho c_p D}\left(T_a-T\right) \tag{1}$$

where T_a is the environmental temperature, which is kept as 5 °C in the simulation. Water vibration is considered as simple harmonic vibration in this model. Fluctuation velocity is the exponential decay with time. Furthermore, the initial amplitude varies with the Reynolds number directly. Fluctuation caused by temperature difference also varies with the Richardson number directly. Therefore, fluctuation velocity could be described:

$$v_p=c_0\,\mathrm{Re}\ln\left(\mathrm{Ri}\right)\mathrm{e}^{-t/\tau_0} \tag{2}$$

where c_0 is effected by the water diffuser structure, τ_0 is related to the fluid characteristic, v_p could be described, with the distance away from inlet as L at time t:

$$v_p\left(L,t\right)=c_0 v\left(t_0\right)\mathrm{e}^{-\Delta t/\tau_0} \tag{3}$$

in which $L=\int_{t_0}^{t} v\mathrm{d}t$, $\Delta t=t-t_0$.

Therefore, the heat storage process is:

$$\frac{\mathrm{d}T}{\mathrm{d}t}=\frac{\lambda}{\rho c_p}\frac{\partial^2 T}{\partial x^2}-v\frac{\partial T}{\partial x}+v_p\frac{\partial T}{\partial x}\bigg|_{+}-v_p\frac{\partial T}{\partial x}\bigg|_{-}+\frac{4K}{\rho c_p D}\left(T_a-T\right) \tag{4}$$

This differential equation is solved by the implicit difference method:

$$\rho A_1\mathrm{d}x c_p\frac{\left(T_i^j-T_i^{j-1}\right)}{\mathrm{d}t}=\frac{\lambda A_1}{\mathrm{d}x}\left(T_{i+1}^j+T_{i-1}^j-2T_i^j\right)+KA_2(T_a-T_i^j)+$$
$$+\left(Q+\rho v_p A_1\right)c_p\left(T_{i-1}^j-T_i^j\right)+\rho v_p A_1 c_p\left(T_{i+1}^j-T_i^j\right) \tag{5}$$

$$T_i^j-T_i^{j-1}=\frac{\lambda}{\rho c_p}\frac{\mathrm{d}t}{\mathrm{d}x^2}\left(T_{i+1}^j+T_{i-1}^j-2T_i^j\right)+\frac{KA_2}{\rho c_p A_1}\frac{\mathrm{d}t}{\mathrm{d}x}(T_a-T_i^j)+$$
$$+\left(\frac{Q}{\rho A_1}+v_p\right)\frac{\mathrm{d}t}{\mathrm{d}x}\left(T_{i-1}^j-T_i^j\right)+v_p\frac{\mathrm{d}t}{\mathrm{d}x}\left(T_{i+1}^j-T_i^j\right) \tag{6}$$

$$T_i^j=\frac{T_i^{j-1}+\frac{\lambda}{\rho c_p}\frac{\mathrm{d}t}{\mathrm{d}x^2}\left(T_{i+1}^j+T_{i-1}^j\right)+\frac{KA_2}{\rho c_p A_1}\frac{\mathrm{d}t}{\mathrm{d}x}T_a+\frac{Q}{\rho A_1}\frac{\mathrm{d}t}{\mathrm{d}x}T_{i-1}^j+v_p\frac{\mathrm{d}t}{\mathrm{d}x}\left(T_{i+1}^j+T_{i-1}^j\right)}{1+2\frac{\lambda}{\rho c_p}\frac{\mathrm{d}t}{\mathrm{d}x^2}+\frac{KA_2}{\rho c_p A_1}\frac{\mathrm{d}t}{\mathrm{d}x}+\frac{Q}{\rho A_1}\frac{\mathrm{d}t}{\mathrm{d}x}+2v_p\frac{\mathrm{d}t}{\mathrm{d}x}} \tag{7}$$

The following equations are relevant at the top of TES tank:

$$\rho A_1\mathrm{d}x c_p\frac{\left(T_1^j-T_1^{j-1}\right)}{\mathrm{d}t}=\frac{\lambda A_1}{\mathrm{d}x}\left(T_2^j-T_1^j\right)+KA_2(T_a-T_1^j)+$$
$$+Qc_p\left(T_{\mathrm{in}}-T_1^j\right)+\rho A_1 v_p c_p\left(T_2^j-T_1^j\right) \tag{8}$$

$$T_1^j-T_1^{j-1}=\frac{\lambda}{\rho c_p}\frac{\mathrm{d}t}{\mathrm{d}x^2}\left(T_2^j-T_1^j\right)+\frac{KA_2}{\rho c_p A_1}\frac{\mathrm{d}t}{\mathrm{d}x}(T_a-T_1^j)+$$
$$+\frac{Q}{\rho A_1}\frac{\mathrm{d}t}{\mathrm{d}x}\left(T_{\mathrm{in}}-T_1^j\right)+v_p\frac{\mathrm{d}t}{\mathrm{d}x}\left(T_2^j-T_1^j\right) \tag{9}$$

$$T_1^j=\frac{T_1^{j-1}+\frac{\lambda}{\rho c_p}\frac{\mathrm{d}t}{\mathrm{d}x^2}T_2^j+\frac{KA_2}{\rho c_p A_1}\frac{\mathrm{d}t}{\mathrm{d}x}T_a+\frac{Q}{\rho A_1}\frac{\mathrm{d}t}{\mathrm{d}x}T_{\mathrm{in}}+v_p\frac{\mathrm{d}t}{\mathrm{d}x}T_2^j}{1+\frac{\lambda}{\rho c_p}\frac{\mathrm{d}t}{\mathrm{d}x^2}+\frac{KA_2}{\rho c_p A_1}\frac{\mathrm{d}t}{\mathrm{d}x}+\frac{Q}{\rho A_1}\frac{\mathrm{d}t}{\mathrm{d}x}+v_p\frac{\mathrm{d}t}{\mathrm{d}x}} \tag{10}$$

Meanwhile, the following equations are relevant at the bottom of the TE tank:

$$\rho A_1\mathrm{d}x c_p\frac{\left(T_N^j-T_N^{j-1}\right)}{\mathrm{d}t}=\frac{\lambda A_1}{\mathrm{d}x}\left(T_{N-1}^j-T_N^j\right)+K\left(A_1+A_2\right)(T_a-T_N^j)+$$
$$+\left(Q+\rho A_1 v_p\right)c_p\left(T_{N-1}^j-T_N^j\right) \tag{11}$$

$$T_N^j-T_N^{j-1}=\frac{\lambda}{\rho c_p}\frac{\mathrm{d}t}{\mathrm{d}x^2}\left(T_{N-1}^j-T_N^j\right)+\frac{K\left(A_1+A_2\right)}{\rho c_p A_1}\frac{\mathrm{d}t}{\mathrm{d}x}(T_a-T_N^j)+$$
$$+\left(\frac{Q}{\rho A_1}+v_p\right)\frac{\mathrm{d}t}{\mathrm{d}x}\left(T_{N-1}^j-T_N^j\right) \tag{12}$$

$$T_N^j = \frac{T_N^{j-1} + \frac{\lambda}{\rho c_p}\frac{\mathrm{d}t}{\mathrm{d}x^2}T_{N-1}^j + \frac{K(A_1+A_2)}{\rho c_p A_1}\frac{\mathrm{d}t}{\mathrm{d}x}T_a + \left(\frac{Q}{\rho A_1}+v_p\right)\frac{\mathrm{d}t}{\mathrm{d}x}T_{N-1}^j}{1+\frac{\lambda}{\rho c_p}\frac{\mathrm{d}t}{\mathrm{d}x^2} + \frac{K(A_1+A_2)}{\rho c_p A_1}\frac{\mathrm{d}t}{\mathrm{d}x} + \left(\frac{Q}{\rho A_1}+v_p\right)\frac{\mathrm{d}t}{\mathrm{d}x}} \tag{13}$$

To obtain c_0 and τ_0 in the disturbance factor, the multi-parameter fitting method is adopted here. These two parameters are fitted based on the experimental results of the heat releasing process.

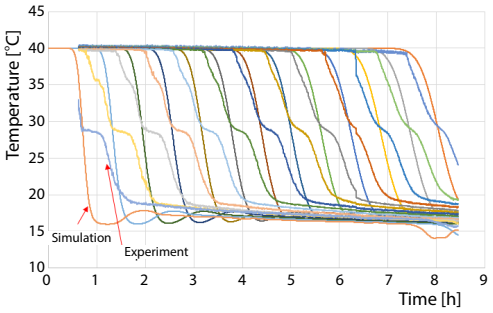

Figure 3. Simulation and experiment comparison without disturbance (heat releasing)

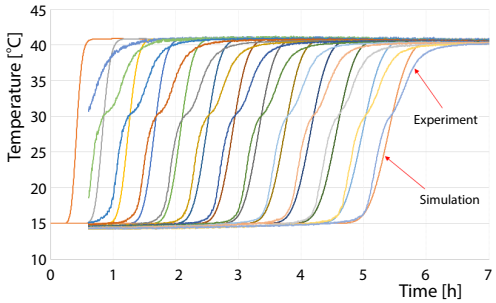

Figure 4. Simulation and experiment comparison without disturbance (heat storing)

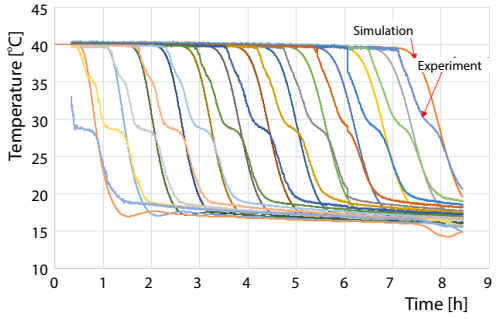

Figure 5. Simulation and experiment comparison with disturbance (heat releasing)

This model is solved with the implicit iteration algorithms, and 700 meshes in the vertical direction with equal intervals divide the TES tank. The iteration precision is 1/700 in the calculation and the time step is 10 seconds in the simulation. The water distributor is just immersed at the top and bottom of the TES tank, thus, there is an initial mixed-layer at the top (heat storing) or at the bottom (heat releasing), where hot water is mixed with cold water directly. Therefore, the initial temperature of the 50 meshes at the top (heat storing) or at the bottom (heat releasing) is the average temperature of the hot water and cold water when considering the thickness of the water distributor. Simulations with and without a disturbance factor are compared to estimate this improved model. Simulation results show better agreement with experiments when considering this disturbance factor. Comparisons without disturbance for heat releasing and heat storing are given in figs. 3 and 4, respectively.

Meanwhile, comparisons with disturbance for heat releasing and heat storing are given in figs. 5 and 6. The disturbance process exists when the hot water or cold water enters the TES tank with a water distributor. This disturbance could obviously affect the development of the temperature profile. Disturbance, conduction, and convection are all considered in this 1-D model, which are necessary key factors for simulation of the temperature profile.

Better agreement between the simulation and experiments is found when applying the disturbance factor. However, there is a significant decrease in the temperature slope between 25 °C and 30 °C, which does not exist in the simulation. Therefore, the mathematical model should be improved with the actual physical model. The water distributor is just immersed at the top and bottom of TES tank as shown in fig. 2,

and the hot water and cold water is mixed directly near the water distributor at the beginning of heat storing or heat releasing process. However, this is not considered in the mathematical model, which is the reason why a significant temperature drop exists. Therefore, the initial temperature of 50 meshes at the top (heat storing) or bottom (heat releasing) is given as the average temperature of hot water and cold water, which could be equal to the thickness of the water distributor. An obvious improvement is found when comparing the simulation and experiment when considering this initial mixed layer, which is shown in fig. 2.

The comparison of the simulation and experiment in terms of the initial mixed-layer is shown in fig. 7, and the initial mixed-layer could explain why a significant temperature drop exists. Furthermore, this temperature drop decreases with time during the experiment, which is also reflected in the simulation.

Better compatibility is found when comparing the simulation and experimental heat storing process, which is shown in fig. 8. This process is reasonable for improving the mathematical model when adding the initial mixed layer.

Simulation analysis

It is found that simulation results show good agreement with experiments when considering the turbulence factor. Therefore, different cases are analysed with this model, which could be applied for TES design.

Fluctuation increases when the temperature difference is larger. Thermocline thickness is often defined as the percent of effective thermocline thickness in the overall temperature difference between inlet and outlet temperatures, which is 80% here. It is found that thermocline thickness is roughly twice as high at 10-80 °C than at 10-20 °C, as shown in fig. 9.

Similar phenomena could also be found with other temperature differences. The thermocline thickness increases mainly due to heat conduction over time. Meanwhile, the turbulence influence weakens at the same time, as shown in fig. 10.

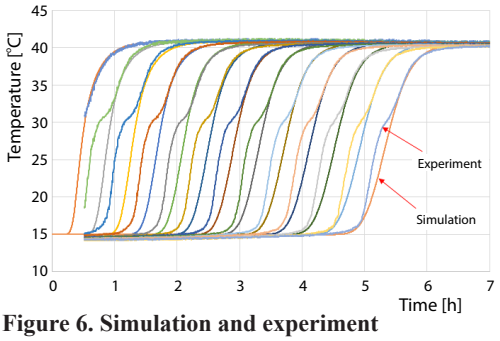

Figure 6. Simulation and experiment comparison with disturbance (heat storing)

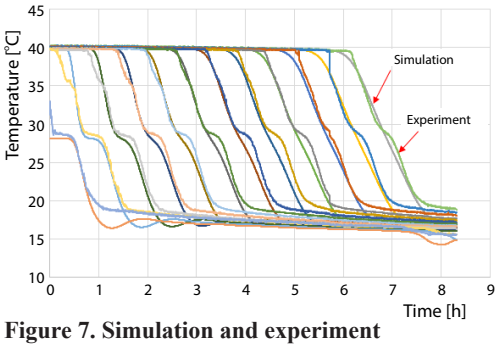

Figure 7. Simulation and experiment comparison with disturbance and initial mixed-layer (heat releasing)

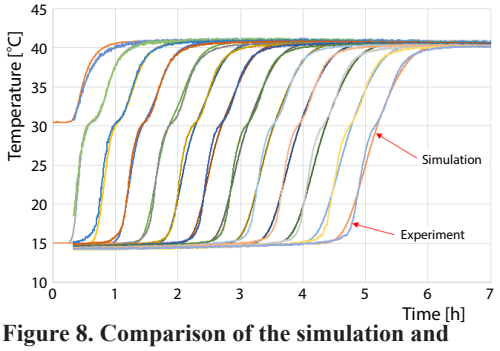

Figure 8. Comparison of the simulation and experimental results with disturbance and the initial mixed-layer (heat storing)

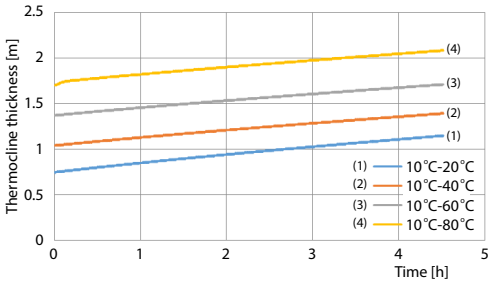

Figure 9. Thermocline thickness at different temperature ranges

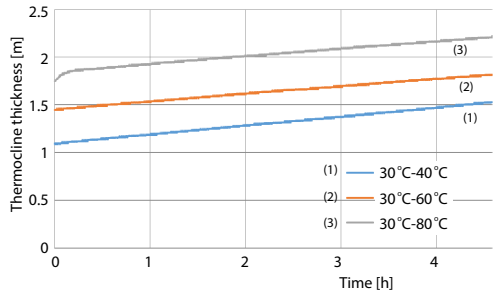

Figure 10. Thermocline thickness at different temperature ranges

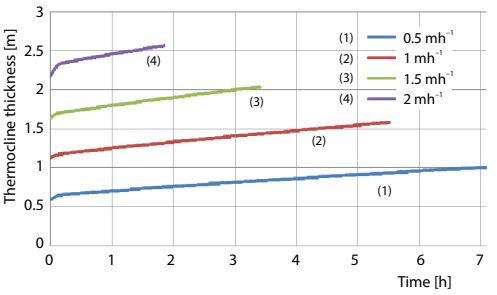

Figure 11. Thermocline thickness with different flow rates

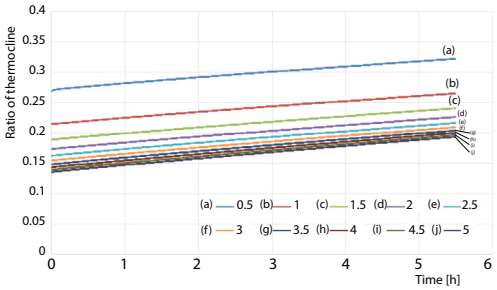

Figure 12. Energy storage efficiency with the height to diameter ratio

The Reynolds number increases when enlarging the water-flow rate. Therefore, thermocline thickness is larger at the beginning. The velocity of the increased thermocline thickness is similar due to the same temperature difference, as shown in fig. 11.

A key parameter in a TES tank is the ratio of height to diameter. Thermocline thickness is reduced with low-temperature differences. Therefore, TES tanks for chilled water storage are often designed with a low height to diameter ratio (<1), which is aimed to reduce material consumption by reducing the pressure of the bottom. However, this ratio is not suitable for tanks with large temperature differences for higher energy storage efficiency. Using the ratio of thermocline to total height, tanks of different sizes with the same volume are compared. It is found that this value increases when the ratio of height to diameter increases. The recommended ratio is 1:2 when considering both the pressure bearing of the tank and the energy storage efficiency, as shown in fig. 12.

Conclusion

An improved model for TES tanks with a large temperature difference including a turbulence factor is given. This factor could reflect the influence of the mixture of hot and cold water with time. Simulation results show good agreement with experimental results when considering the fluctuation influence. Fluctuation increases when the temperature difference increases. Thermocline thickness increases when the Reynolds number increases. The height to diameter ratio is often less than one when adopted for cold-water storage due to the small temperature difference. However, energy storage efficiency is reduced significantly for a TES tank with a large temperature difference with this ratio. Therefore, 1:2 is the ratio recommended for large temperature differences (>25 °C).

Acknowledgment

The authors are grateful for the support provided by the National Natural Science Funds of China (51606061), and thanks are also given to anonymous reviewers for their comments on this manuscript.

Nomenclature

A – area, [m^2]

c_p – specific heat of constant pressure, [Jkg^{-1}K^{-1}]

D – diameter of TES, [m]
g – acceleration of gravity, [ms^{-2}]
K – coefficient of thermal conductivity, [Wm^{-1}K^{-1}]
L – characteristic length, [m]
Q – flow rate, [kgs^{-1}]
Re – Reynolds number (= VDv^{-1}), [–]
Ri – Richardson number (= g$\beta\Delta TLV^{-2}$), [–]
T – temperature, [°C]
T_a – environmental temperature, [°C]
ΔT – temperature difference, [°C]
t – time, [s]
V – velocity of water, [ms^{-1}]

Greek symbols

β – coefficient of cubic expansion
λ – thermal conductivity, [m^{-1}K^{-1}]
ρ – density, [kgm^{-3}]
ν – kinematic viscosity, [m^{2}s^{-1}]

Acronyms

AHP – absorption heat pump
EHP – electric heat pump
TES – thermal energy storage

References

[1] Jiang, Y., *Annual Report of China Building Energy Conservation*, China Architecture and Building Press., Beijing, China, 2015
[2] Sun, F. T., *et al*., New Waste Heat District Heating System with Combined Heat and Power Based on Absorption Heat Exchange Cycle in China, *Appl. Therm. Eng.*, 37 (2012), May, pp. 136-144
[3] Sun, J., *et al*., Experimental Study on a Project with CHP System Basing on Absorption Cycles, *Appl. Therm. Eng.*, *73* (2014), 1, pp. 730-736
[4] Schmidt, T., *et al*., Central Solar Heating Plants with Seasonal Storage in Germany, *Sol. Energy.*, *76* (2004), 1-3, pp. 165-174
[5] Lund, H., *et al*., From Electricity Smart Grids to Smart Energy Systems a Market Operation Based Approach and Understanding, *Energy.*, *42* (2012), 1, pp. 96-102
[6] Streckiene, G., *et al*., Feasibility of CHP-Plants with Thermal Stores in the German Spot Market, *Appl. Energy.*, *86* (2009), 11, pp. 2308-2316
[7] Harris, M., Thermal Energy Storage in Sweden and Denmark, M. Sc. thesis, Lund University, Lund, Sweden, 2011
[8] Bauer, D., *et al*., German Central Solar Heating Plants with Seasonal Heat Storag, *Sol. Energy.*, *84* (2010), 4, pp. 612-623
[9] Potter, R., Study of Operational Experience with Thermal Storage Systems, Report No. 766, Atlanta, Geo., USA, 1995
[10] Han, Y. M., *et al*., Thermal Stratification within the Water Tank, *Renew. Sust. Energ. Rev.*, *13* (2009), 5, pp. 1014-1026
[11] Shin, M. S., *et al*., Numerical and Experimental Study on the Design of a Stratified Thermal Storage Syste, *Appl. Therm. Eng.*, *24* (2003), 1, pp. 17-27
[12] Consul, R., Virtual Prototyping of Storage Tanks by Means of Three-Dimensional CFD and Heat Transfer Numerical Simulations. *Solar. Energy.*, *77* (2004), 1, pp. 79-91
[13] Ghajar, A. J., Zurigat, Y. H., Numerical Study of the Effect of Inlet Geometry on Stratification in Thermal Storage, *Numer. Heat. Tr. A.*, *19* (1991), 1, pp. 65-83
[14] Ismail, K. A. R., *et al*., Models of Liquid Storage Tanks, *Energy.*, *22* (1997), 8, pp. 805-815
[15] Karim, M. A., Experimental Investigation of a Stratified Chilled-Water Thermal Storage System. *Appl. Therm. Eng., 31* (2011), 11-12, pp. 1853-1860
[16] Rejane, D. C. O., *et al*., Comparison between Models for the Simulation of Hot Water Storage Tanks, *Solar. Energy.*, *75* (2003), 2, pp. 121-134
[17] Angrisani, G., *et al*., Calibration and Validation of a Thermal Energy Storage Model: Influence on Simulation Results, *Appl. Therm. Eng,. 67* (2014), 2, pp. 190-200
[18] Rahman, A., *et al*., Simplified Modeling of Thermal Storage Tank for Distributed Energy Heat Recovery Applications, *Proceedings,* ASME 2015 Power and Energy Convers Conf., San Diego, Cal., USA, 2015, Vol. 2, No. 49170
[19] Kleinbach, E., *et al*., Performance Study of one Dimensional Models for Stratified Thermal Storage Tanks, *Sol. Energy.*, 50 (1993), 2, pp. 155-166

Paper submitted: July 20, 2016
Paper revised: May 17, 2017
Paper accepted: August 4, 2017